Received: 31 October 2019 | Accepted: 23 March 2020 | Published online: 18 July 2020

DOI: 10.1002/saj2.20071

Soil Science Society of America Journal

NUTRIENT MANAGEMENT & SOIL & PLANT ANALYSIS

Optimization of measuring procedure of farmland soils using laser-induced breakdown spectroscopy

Xuebin Xu[1,2] | **Changwen Du**[1,2] | **Fei Ma**[1] | **Yazhen Shen**[1] | **Yiqiang Zhang**[3] | **Jianmin Zhou**[1]

[1] State Key Laboratory of Soil and Sustainable Agriculture, Chinese Academy of Sciences, Institute of Soil Science, Nanjing 210008, China

[2] University of Chinese Academy of Sciences, Beijing 100049, China

[3] Water Conservancy Research Institute of Bayannur City, Bayannur 015000, China

Correspondence
Du Changwen, State Key Laboratory of Soil and Sustainable Agriculture, Institute of Soil Science, Chinese Academy of Sciences, Nanjing 210008, China.
Email: chwdu@issas.ac.cn

Funding information
"STS" Project from Chinese Academy of Sciences, Grant/Award Numbers: KFJ-PTXM-003, KFJ-STS-QYZX-047; National Natural Science Foundation of China, Grant/Award Numbers: 41671238, 41977026; Jiangsu Demonstration Project in Modern Agriculture, Grant/Award Number: BE2017388

Abstract

Laser-induced breakdown spectroscopy (LIBS) is an emerging multi-elemental analytical technique offering fast and simultaneous quantification of soil properties with minimal sample preparation and effective cost. Due to soil heterogeneity, spectral variation however limits the quantitative robustness. In this study, 348 soil samples were collected and prepared for acquisition of LIBS spectra. Influences of shot layer and number on LIBS quality were evaluated by spectral intensity and relative standard deviation (RSD). Effects of shot layer and number and five normalization procedures on LIBS ability to measure soil organic matter (SOM), total nitrogen (TN), and total soluble salt content (TSC), were evaluated using partial least squares regression (PLSR). Increasing shot number reduced LIBS spectral variance, thereby improving the quantitative accuracy of selected soil properties. Deep shot layers (4th or 5th shot layers) reduced the intensities of soil spectra and thereby decreased the quantitative accuracy for TSC. However, deep shot layers improved the SOM and TN prediction performances. Among the normalization approaches, the method based on the correction of Si line (DS) showed superior performance for improving quantitation of SOM and TN. The arithmetic average method (AA) was best for TSC prediction. Optimization of shot layer, number and normalization procedures of LIBS spectra resulted in fair prediction of SOM (residual prediction deviation of validation set, $RPD_V = 1.608$), good prediction of TN ($RPD_V = 1.836$), and very good quantitative analysis of TSC ($RPD_V = 2.456$). Therefore, our findings illustrate very good potential for improving the quantitative accuracy of the LIBS soil spectra.

1 | INTRODUCTION

The key aspect of accomplishing accurate management of soil nutrients in precision agriculture is the recognition of local changes in the soil environment within traditional management units and then addressing them appropriately (Ji et al., 2019). However, conventional laboratory-based soil analytical methods have been used in an attempt to establish the relationship between soil physical

Abbreviations: AA, arithmetic average method; DA, method based on the correction of spectral area; DM, method based on the correction of spectral maximum; DN, method based on the correction of spectral norm; DS, method based on the correction of Si line; LIBS, laser-induced breakdown spectroscopy; nLV, number of latent variables; PLSR, partial least squares regression; $RMSE_{CV}$, root-mean-square-error of cross-validation; $RMSE_V$, root-mean-square-error of validation set; RPD_V, residual prediction deviation of validation set; RSD, relative standard deviation; SOM, soil organic matter; TN, total nitrogen; TSC, total soluble salt content; VIP, variable important in projection.

and chemical properties and individual soil components, often ignoring their complex, multi-component interactions (Ma, Du, & Zhou, 2016). Moreover, these conventional methods are time- and cost-consuming, tedious, destructive to the sample being analyzed, and sometimes generate toxic waste that must be disposed of correctly (Ma, Du, Zhou, & Shen, 2019; Peltre, Bruun, Du, Thomsen, & Jensen, 2014). Therefore, the development of fast, cost-efficient, and convenient methodologies to estimate soil properties will be of great significance for monitoring and evaluating soil conditions and understanding their complex and multi-component interactions.

Laser-induced breakdown spectroscopy is a multi-elemental spectroscopic technique based on atomic emission spectroscopy. By focusing a high-energy laser beam on the sample surface, a plasma generates the atomic emission of elements. This technique shows great potential for soil analysis because it is rapid, quasi-nondestructive, and produces real-time multi-elemental measurements (Luna, Gonzaga, da Rocha, & Lima, 2018; Paules et al., 2018). Furthermore, the simple structure of LIBS systems allows for design of portable devices for field use (Knadel et al., 2017; Yamamoto, Cremers, Ferris, & Foster, 1996). Previous studies have reported the application of LIBS for quantitative analysis of soil properties, including soil texture (Villas-Boas et al., 2016), pH (Ferreira, Neto, Milori, Ferreira, & Anzano, 2015), CEC (Liu, Zeng, Zhang, Liu, & Lin, 2012), C (Cremers et al., 2001; Martin et al., 2010; Nguyen, Moon, & Choi, 2015), and N, P, and K (Dong, Zhao, Zheng, Zhao, & Jiao, 2013; Lu et al., 2013).

However, the application of LIBS in measurements of soil properties is limited by the matrix effect and poor repeatability which results in poor precision and sensitivity (Hao et al., 2018). The matrix effect is caused by changes in the emission line intensities of some elements in samples when the physical properties and the chemical composition of the matrix vary (Senesi, 2014). Several attempts to improve the quantitative accuracy of LIBS and reduce the matrix effect using chemometrics and multivariate methods have been made (Eppler, Cremers, Hickmott, Ferris, & Koskelo, 1996; Takahashi & Thornton, 2017; Zaytsev, Krylov, Popov, Zorov, & Labutin, 2018). Poor precision caused by highly variable measurements is a concern. Causes include pulse fluctuation, the distance of plasma light to the collection fiber, scattering of light, atmospheric conditions, variation of the lens to sample distance, and material homogeneity (Michel & Chave, 2007; Motto-Ros, Negre, Pelascini, Panczer, & Yu, 2014). Several studies indicate that the optimization of LIBS parameters contributed to an improvement of the signal repeatability (Fu, Hou, Li, Li, & Wang, 2019; Hao et al., 2018; Sirven, Mauchien, & Sallé, 2008). In addition, spectral normalization methods are proven to be an effective strategy for enhancing the repeatability of the LIBS signal (Body & Chadwick, 2001; Hao et al., 2018). Soil is heterogeneous because of the uneven distribution of soil components in a microscale space. The laser spot focused on the soil surface is sometimes smaller than the diameter of some aggregates in the soil. Consequently, variations of the spectra at each site are significantly different. The signal variation caused by the inhomogeneity of a soil sample is mainly responsible for the low repeatability of the LIBS signal (Wainner, Harmon, Miziolek, McNesby, & French, 2001).

Precision also depends on soil preparation and LIBS measurement processes. In the LIBS measurement process, shot layer and number are the main factors affecting the repeatability of LIBS soil spectra. A LIBS spectrum is attained by one ablation or shot of the laser in the vertical plane at a specific site of the sample. At a specific site, an initial crater with certain depth is produced after the first ablation and this ablation is called the first shot layer. Then the second ablation is created on the bottom of the initial crater to produce a deeper crater and this second ablation is called the second shot layer. By that analogy, spectra of different shot layers are obtained. Unfortunately, the optimization of shot layer and number for LIBS soil spectra remain unknown. Moreover, we hypothesize that both optimization of shot layer and number and data normalization methods may benefit the accuracy of LIBS for quantifying soil properties. Therefore, these combined effects on the quantitative accuracy of LIBS soil spectra deserve an in-depth investigation.

In this work, we applied the LIBS technique at different shot numbers to acquire LIBS soil spectra for 348 soil samples collected from Hetao Irrigation District, China. Several types of spectral normalization methods were applied to preprocess the spectra of multiple measurements. A PLSR model was used to assess the ability of LIBS soil spectra to quantitatively analyze SOM, TN, and TSC. The objectives of this study were to: (i) evaluate the influences of shot layer and number on the quality of LIBS soil spectra; (ii) evaluate the influences of shot layer and number and

Core ideas

- LIBS is an emerging multi-elemental analytical technique for soil samples.
- Soil heterogeneity resulted in the limitation of LIBS application in soil analysis.
- Optimization of laser shots improved the representation for heterogeneous soil samples.
- Spectra normalization strategies increased the detection accuracy through removing interferences.

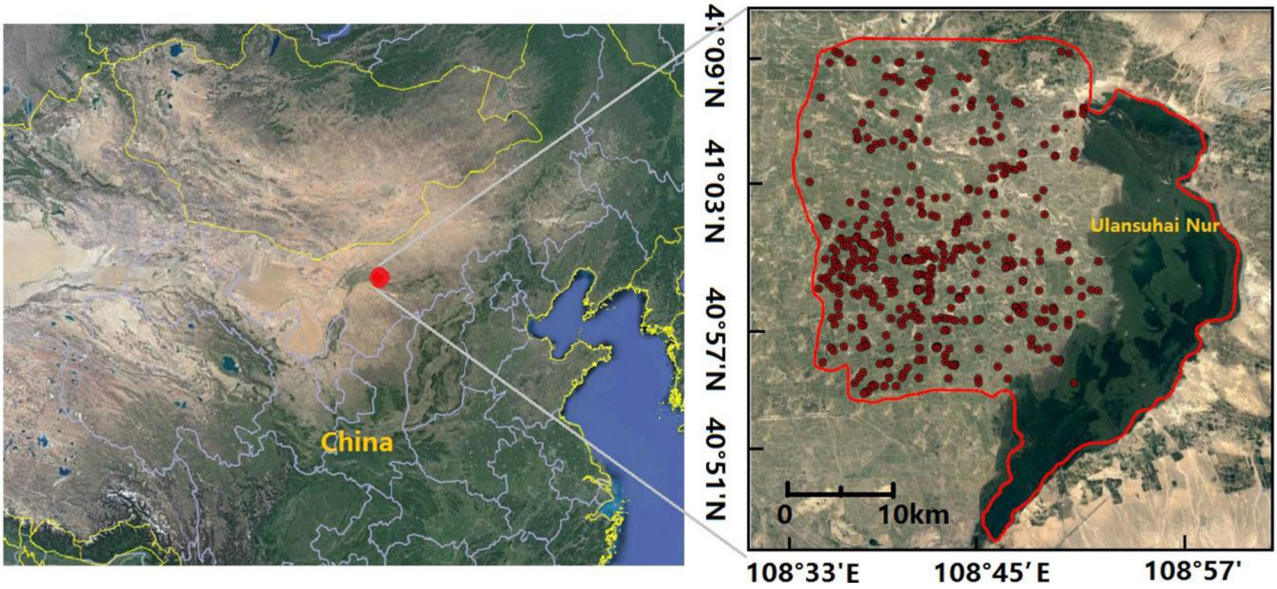

FIGURE 1 Distribution map of the soil sampling sites in this study

spectra normalization methods on the quantitative analysis using LIBS soil spectra; and (iii) optimize the combination of shot layer and number and spectral normalization methods for improving the quantitative abilities of LIBS soil spectra.

2 | MATERIALS AND METHODS

2.1 | Study area

The study area was located in Urad Front Banner, Inner Mongolia, in northern China (Figure 1). This region is the third-largest irrigation district in China, covering a total area of 1.12×10^6 ha (Feng, Wang, & Feng, 2005). As a typical arid continental climate, the mean annual precipitation in this region is 150 mm and the mean annual potential evaporation is in the range of 2200–2400 mm (Lei, Issac, Yuan, Huang, & Yang, 2001). As a result, crop production in this region relies heavily on flood irrigation using water diverted from the Yellow River (Yang, Shang, & Jiang, 2012). The soil texture is a silty clay loam with severe salinization (Yu et al., 2010). Soils are Aridisols according to the USDA soil taxonomic system (Yue, Guo, Lin, Li, & Zhao, 2016). Local crops are mainly spring wheat (*Triticum aestivum* L.), sunflower (*Helianthus annuus* L.), and maize (*Zea mays* L.) (Chen et al., 2018).

2.2 | Soil sampling and chemical analysis

In 2015, a total of 348 topsoil samples (0- to 20-cm depth) were collected from farmland with the precise location determined using GPS. Soil samples were collected at 348 randomly selected locations (Figure 1) using a 35-mm soil auger after the autumn irrigation. The soils were fully mixed and stored in plastic sampling bags for subsequent analysis. Before laboratory analysis, the soil samples were air-dried at room temperature and were then passed through a 2-mm sieve. Content of SOM was determined using a potassium dichromatic oxidation titration method (Walkley & Black, 1934). Content of TN was determined using the Kjeldahl method, with a Kjeldahl analyzer (Kjeltec 8200, FOSS Analytical, Hilerod, Denmark) (Pansu & Gautheyrou, 2007). Total soluble salt was extracted using a 1:5 soil/water suspension and the cation and anion content were determined by the method described by Lao (1988). Briefly, 50 ml of extract was dried by distillation using a water bath. Then aliquots of 15% H_2O_2 were added repeatedly to remove the OM as visually observed. The residue was subsequently oven-dried to constant weight at 105°C. The TSC was calculated by the amount of residue, volume of extract and soil to water ratio.

2.3 | Sample preparation and spectral acquisition

Before the spectral acquisition, soil samples of approximately 0.5 g were pelletized to dimensions of 1-cm diameter and 0.25-cm thickness with an applied pressure of ~55 MPa for 2 min using a tablet machine (YP-2, Tianjin, China). The pelletized soil tablets were placed over an X–Y–Z manual/automatic, micro-metric platform with a 1.0-μm stage of travel at every coordinate. Various spectral acquisition approaches were achieved according

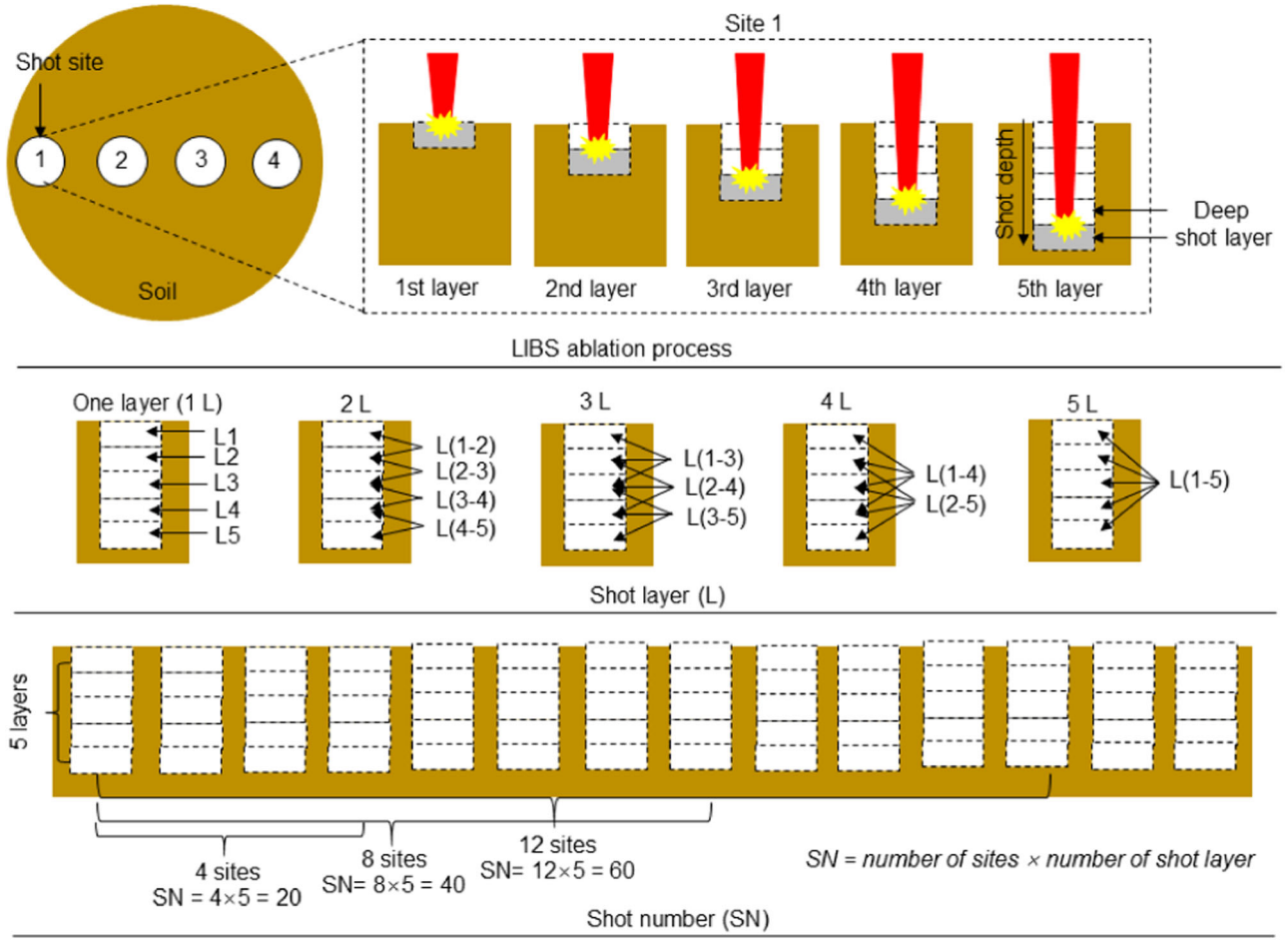

FIGURE 2 Schematic diagram of LIBS ablation process and the relationship between shot layer and number

to the combination of different shot layers and numbers (Figure 2). The LIBS laser first produced an initial ablation crater on the surface of soil pellet and this ablation was the first shot layer. Then the laser sequentially ablated on the bottom of the initial crater to produce a deeper crater and this second ablation was the second shot layer. As an analogy, *m* spectra of *m* shot layers at one specific site were obtained. After that, the laser moved to a fresh site to repeat the above process until *n* shot sites were achieved. Thus, the shot number and total number of spectra for one sample was $m \times n$. The *i*th shot layer of all sites was labeled as L*i* and the *i*th to *j*th shot layers of all sites were labeled as L(*i*-*j*). The *k* shot number was labeled as SN*k*. The combinations of different shot layer and number were labeled as L(*i*-*j*)/SN*k*. For example, the first to fourth shot layers with a total of 80 shot numbers (20 sites, 4 shots/site) was labeled as "L(1-4)/SN80". The shot depth refers to the depth from the crater of the shot layer to the surface of soil pellet. The 1st and 2nd shot layers are considered as surface shot layers and 4th and 5th shot layers are considered as deep shot layers. Spectra obtained under different combinations of shot layer and number were used for subsequent spectral processing and modeling. In particular, for the three shot layers' condition, one and two spectra of the third layer were removed for keeping the shot number at 20 and 40, respectively, before subsequent spectral processing and modeling.

A MobiLIBS system (IVEA, Orsay, France) with AnaLibs control software was used for spectral acquisition. A fourth-harmonic Nd:YAG laser (Quantel, Paris, France) was operated at 266 nm with a 5-ns pulse duration, to generate a laser beam with the frequency of 20 Hz and delivery energy of 16 mJ. The laser beam was focused on the pelleted sample with a spot/site diameter of 50 μm by a lens with a focal length of 15 cm. A plasma was produced in the ablation area and light radiated during plasma cooling. Emitted light was collected by a collection lens and transmitted to a Mechelle 5000 Echelle spectrometer (Andor Technology, Ltd., Belfast, Northern Ireland) by a fiber optic cable. The resolving power of this spectrometer ($\lambda/\Delta\lambda$) is 4,000. An intensified charge-coupled device camera (iStar, Andor Technology, Ltd.) was used to collect the diffracted light. The delay time and the gate width were controlled and adjusted to the optimal conditions

(370 μs delay time and 7.0 ms gate width) in advance. The wavelengths of the obtained spectra ranged from 200 to 1000 nm and the resolution was 0.116 nm.

2.4 | Baseline correction and outlier removal of spectra

The baseline drift of the LIBS spectra was corrected using a morphological-weighted penalized least squares (MPLS) algorithm (Li et al., 2013). The MPLS algorithm can be briefly described as: (i) a rough background profile was first obtained using a mathematical morphological opening operation; (ii) the rough background and the local minimum values were then used as the input vector for penalized least squares to refine the background profile; and (iii) the corrected spectrum was obtained by subtracting the refined background profile from the original spectrum. In this work, the adjustable parameters, λ and window size, in the MPLS algorithm were set as 10,000 and 100, respectively. After baseline correction, a principal component analysis (PCA) was performed on the spectra to remove spectral outliers that existed in multiple measurements for each soil sample. The spectra with the first principal component (PC1) scores of below −10,000 were identified as outliers and were removed.

2.5 | Spectral normalization methods

Castro and Pereira-Filho (2016) applied twelve normalization methods to reduce the interference matrix and improve the calibration models. Some of their normalization methods showed great improvement for calibration of metal elements in alloys. In this study, normalization approaches were selected to normalize the LIBS spectra with repeated measurements for each sample (Castro & Pereira-Filho, 2016), consisting of the following methods:

(1) The arithmetic average was calculated for the spectra over a number of measurements and this method was labeled as AA.
(2) Each repeated spectrum was divided by its individual norm and the norm of each repeated spectrum of was assigned a value of 1. The AA of the normalized spectra was then calculated. This normalization method was labeled as DN.
(3) Each repeated spectrum was divided by its individual spectral area and the area of each repeated spectrum was assigned a value of 1. The AA of the normalized spectra was then calculated. This normalization method was labeled as DA.
(4) Each repeated spectrum was divided by its spectral maximum (the highest signal) and the signal intensity of the highest emission line for each repeated spectrum was assigned a value of 1. The AA of the normalized spectra was then calculated. This normalization method was labeled as DM.
(5) Each repeated spectrum was divided by the signal intensity of Si I 287.9 nm and the signal intensity of Si I 287.9 nm for each repeated spectrum was assigned a value of 1. The AA of the normalized spectra was then calculated. This normalization method was labeled as DS.

2.6 | Partial least squares regression and model evaluation

Partial least squares regression is a widely used modeling approach as it can be used to analyze data where there are multiple **X** variables that are strongly collinear (correlated) and noisy (Wold, Sjöström, & Eriksson, 2001). In PLSR, a vector, **y** (SOM, TN, or TSC), can be described as a function of the elements of **X** (spectra) for predictions using the smallest number of latent variables (nLV). In the present study, PLSR was used to evaluate the effects of different spectral acquisition and normalization approaches on the quantitative accuracy of LIBS soil spectra. The nLV in PLSR was optimized by ten-fold cross-validation. The optimal number of LVs was determined when the local minimum of root-mean-square-error of cross-validation ($RMSE_{CV}$) was achieved. Spatial autocorrelation analysis in ArcGIS v10.2 (ESRI, California, USA) showed that all *p* values of the spatial autocorrelation for SOM, TN, and TSC were greater than 0.05. This indicated that the SOM, TN, and TSC were spatially independent. Therefore, the full spectra dataset was randomly divided into a calibration set (75%, 261 samples) and a validation set (25%, 87 samples). The calibration set was used for modeling PLSR and the validation set was used for verifying the prediction performance. The statistics of chemically measured contents of SOM, TN, and TSC in the calibration and validation sets are presented in Table 1. To evaluate the repeatability of measurements, robustness, and accuracy of the model, RSD of various spectral lines, the coefficients of determination (R^2), root-mean-square-error of validation set ($RMSE_V$), and RPD_V of prediction were determined (Xing et al., 2016). These evaluation parameters were specifically defined by the following formulae:

$$\mathrm{RSD} = \frac{\sqrt{\frac{\sum_{j=1}^{n}(x_j-\bar{x})^2}{n-1}}}{\bar{x}} \times 100\% \quad (1)$$

TABLE 1 Statistics of soil organic matter (SOM), total nitrogen (TN), and total soluble salt content (TSC) measured by the reference chemical methods

Properties	N	Range	Median	Mean	SD[a]	CV[b]
		g kg^{-1}				%
All soil samples						
SOM	348	5.37–21.00	13.00	13.08	3.01	23.04
TN	348	0.27–1.24	0.82	0.80	0.87	23.48
TSC	348	0.44–7.54	0.90	1.24	1.00	81.21
Calibration set						
SOM	261	5.37–21.00	13.10	13.32	2.86	21.47
TN	261	0.32–1.24	0.82	0.81	0.17	20.99
TSC	261	0.44–6.54	0.89	1.14	0.8	70.18
Validation set						
SOM	87	6.21–19.50	12.20	12.37	3.36	27.16
TN	87	0.27–1.12	0.79	0.76	0.23	30.26
TSC	87	0.54–7.54	0.93	1.43	1.2	83.92

[a]SD, standard deviation.
[b]CV, coefficient of variation.

$$R^2 = 1 - \frac{\sum_{i=1}^{N}(y_i - \hat{y}_i)^2}{\sum_{i=1}^{N}\left(y_i - \bar{\hat{y}}\right)^2} \quad (2)$$

$$\mathrm{RMSE_V} = \sqrt{\frac{1}{N}\sum_{i=1}^{N}(y_i - \hat{y}_i)^2} \quad (3)$$

$$\mathrm{RPD_V} = \frac{\mathrm{SD}}{\mathrm{RMSE_V}} \quad (4)$$

$$\mathrm{SD} = \sqrt{\frac{1}{N}\sum_{i=1}^{N}(y_i - \bar{y})^2} \quad (5)$$

where n is the number of repeated measurements; x_j is the spectral intensity of jth repeated measurement; $\bar{x}$ is the average intensity of n repeated spectra; y_i and $\hat{y}_i$ refer to the measured value and the corresponding estimated value, respectively; $\bar{\hat{y}}$ is the average of the estimated value; N denotes the number of observations; and $\bar{y}$ is the average of the measured value. The $\mathrm{RPD_V}$ value in soil science is considerably lower than in most other fields because of the complicated interaction among soil components, which influences the distribution of specific soil properties (Du, Ma, Zhou, & Goyne, 2013). Thus, $\mathrm{RPD_V}$ values < 1.4 were considered poor; those ≥ 1.4 and < 1.8 were considered fair and allowed the model prediction to be used for assessment and correlation; those ≥ 1.8 and < 2.0 were considered good, in which case quantitative predictions were possible; those ≥ 2.0 and < 2.5 were considered very good for quantitative analysis; and those ≥ 2.5 were considered excellent (Lu, Du, Yu, & Zhou, 2014; Rossel, McGlynn, & McBratney, 2006).

The variable importance in projection (VIP) in PLSR was used to determine the interpretative ability of spectral lines for soil properties (Farrés, Platikanov, Tsakovski, & Tauler, 2015). The VIP score for the kth variable is given as

$$\mathrm{VIP}_k = \sqrt{\frac{\sum_{k}^{F} w_{kf}^2 \mathrm{SSY}_f \, \mathrm{J}}{\mathrm{SSY}_T \, \mathrm{F}}} \quad (6)$$

where w_{kf} is the weight value for the kth variable and f latent variable in PLSR; SSY_f is the sum of squares of explained variance for the fth latent variable and J is the number of spectral variances. The term $\mathrm{SSY_T}$ is the total sum of squares explained by the dependent variance; and F is the total number of latent variables. The Spearman correlations between the $\mathrm{RMSE_V}$ values of SOM, TN, and TSC and the RSD of various element lines (C, N, K, Ca, Mg, and Si) were used to assess the influence of the RSD values of various element lines on the quantitative accuracy. All above statistical and spectral analyses were implemented in MATLAB R2016a software (MathWorks, Natick, MA, USA).

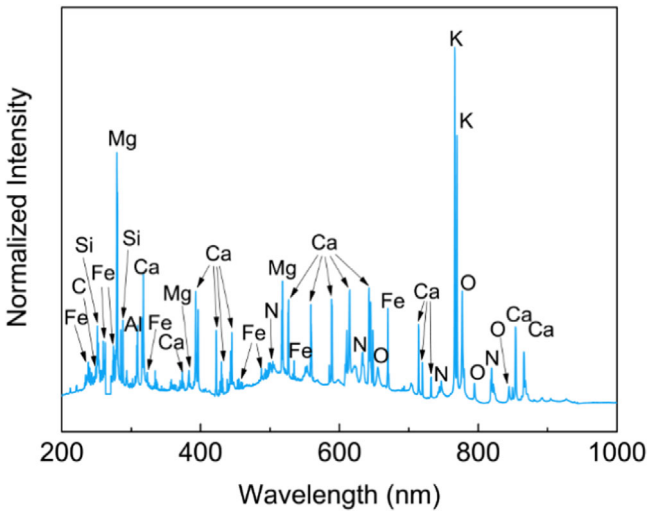

FIGURE 3 Preprocessed LIBS spectra of farmland soils

3 | RESULTS

3.1 | Soil properties

The descriptive statistics of the soil properties are listed in Table 1. The SOM content of the 348 soil samples ranged from 5.37 to 21.00 g kg^{-1}, with median and mean content of 13.00 and 13.08 g kg^{-1}, respectively. The TN content ranged from 0.27 to 1.24 g kg^{-1}, with median and mean content of 0.82 and 0.80 g kg^{-1}, respectively. The TSC of samples ranged widely from 0.44 to 7.54 g kg^{-1}, with median and mean content of 0.90 and 1.24 g kg^{-1}, respectively, indicating the existence of a small number of soil samples with high TSC.

3.2 | Features of LIBS soil spectra

The average LIBS spectrum of the 348 soil samples displayed various responses to atomic emission at different wavelengths from 200 to 1000 nm (Figure 3). The C I emission line was observed at 247.8 nm (Cremers et al., 2001). The signals at 343.7, 498.2, 498.9, 499.9, 500.6, 501.6, 503.0, and 633.1 nm were attributed to the emission lines of N II (Harris, Cremers, Ebinger, & Bluhm, 2004); and the signals at 742.3, 744.2, 746.8, 818.25, 819.3, 821.7, and 824.3 nm were attributed to N I emission lines (De Lucia Jr & Gottfried, 2010; Dong et al., 2013; Harris et al., 2004). The O I emission lines were observed at 777.1 and 844.6 nm; the O II emission line was observed at 655.6 nm; and the O III emission line was observed at 794.6 nm (Ji, Xi, & Mao, 2010). The strong emission lines at 766.3 and 769.8 nm corresponded to the emission of K I (Mansoori, Roshanzadeh, Khalaji, & Tavassoli, 2011; Sallé, Cremers, Maurice, Wiens, & Fichet, 2005). Abundant Ca emission lines were observed, including Ca I emission lines at 422.5, 429.8, 445.4, 526.4, 558.8, 615.6, 645.1, 714.8, and 720.2 nm; Ca II emission lines at 315.7, 317.7, 373.5, 393.0, 396.5, 732.3, 854.2, and 866.2 nm; and Ca III emission lines at 642.5 and 648.3 nm (Ahmed, Umar, Ahmed, & Baig, 2017; Juvé, Portelli, Boueri, Baudelet, & Yu, 2008; Velioglu, Sezer, Bilge, Baytur, & Boyaci, 2018; Yaroshchyk, Morrison, Body, & Chadwick, 2005). Several signals at 279.3 and 280.0 nm were attributed to Mg II emission lines and those at 382.9 and 383.5 nm represented Mg I emission lines (Abdel-Salam, Al Sharnoubi, & Harith, 2013; Li, Liu, Chen, & Li, 2008; Mansoori et al., 2011; Rai, Zhang, Yueh, Singh, & Weisberg, 2001; Yaroshchyk et al., 2005; Zheng et al., 2008). An Al I emission line was observed at 309.2 nm (Mansoori et al., 2011; Yaroshchyk et al., 2005). Two Si I emission lines were observed at 251.4 and 287.9 nm (Ismail et al., 2006; Juvé et al., 2008; Mansoori et al., 2011; Sabsabi, Detalle, Harith, Tawfik, & Imam, 2003; Zheng et al., 2008). In addition, numerous Fe I and II emission lines were observed at 460.6 and 487.7 nm and 237.1, 259.7, 262.8, 274.4, 323.2, 534.7, and 669.9 nm, respectively. The characteristic emission lines of C, O, and N corresponding to SOM; N and O corresponding to TN; and C, O, Ca, Mg, and K corresponding to TSC can be clearly observed and distinguished, indicating the theoretical feasibility of this method for quantitative analysis.

3.3 | Effects of the spectral acquisition approaches on the quality of LIBS soil spectra

The average intensity and RSD of C (247.8 nm), N (460.5 nm), K (766.1 nm), Ca (393.0 nm), Mg (279.1 nm), and Si (287.9 nm) lines were used to estimate the effects of shot layer and number. The boxplots of the average intensity of C, N, K, Ca, Mg, and Si lines in the 348 soils with the different shot layers are found in Figure 4. The average intensity of C, N, K, Ca, Mg, and Si lines decreased with increasing of shot layer both in one, two, three, and four layer conditions, suggesting low LIBS intensity with deep shot layers. However, the variation in the average intensity among the 348 soils was reduced with increasing shot depth. The boxplots of the RSD of C, N, K, Ca, Mg, and Si lines in these soils with the different shot layers are shown in Figure 5. The RSD values of these spectral lines increased with increasing shot layer except for the C line, which indicated that the shot-to-shot signal variation for each soil increased with the shot depth.

The mean values of the C, N, K, Ca, Mg, and Si intensities in the 348 soil samples did not vary as shot number increased (Figure 6). The interquartile ranges of the C, N, K, Ca, Mg, and Si intensities among these soil samples decreased along with the increase of shot number

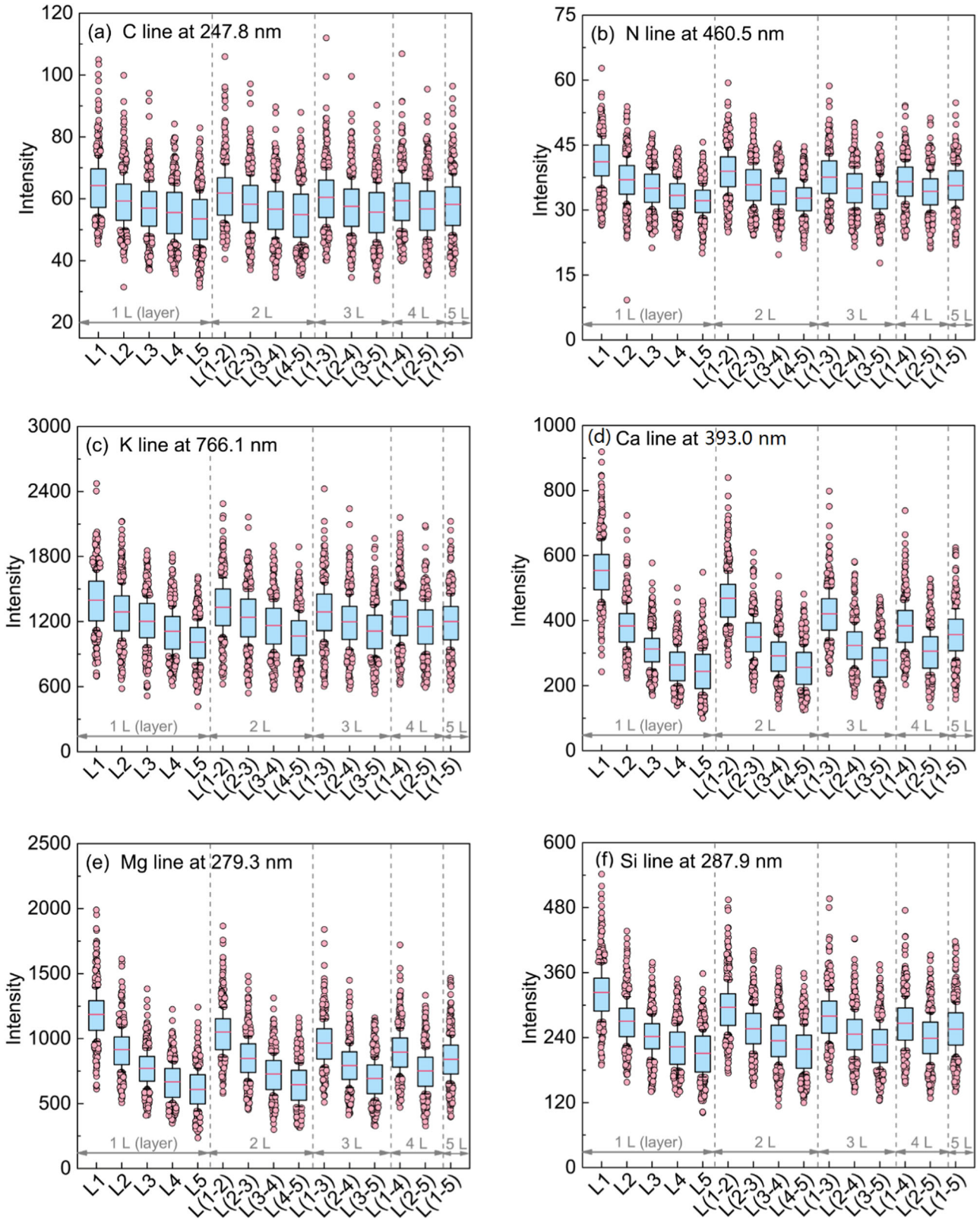

FIGURE 4 Boxplots of the LIBS intensity of (a) C, (b) N, (c) K, (d) Ca, (e) Mg, and (f) Si lines among 348 soil samples as a function of different shot layers. The number labeled after "L" denotes the shot layer; shot number = 20

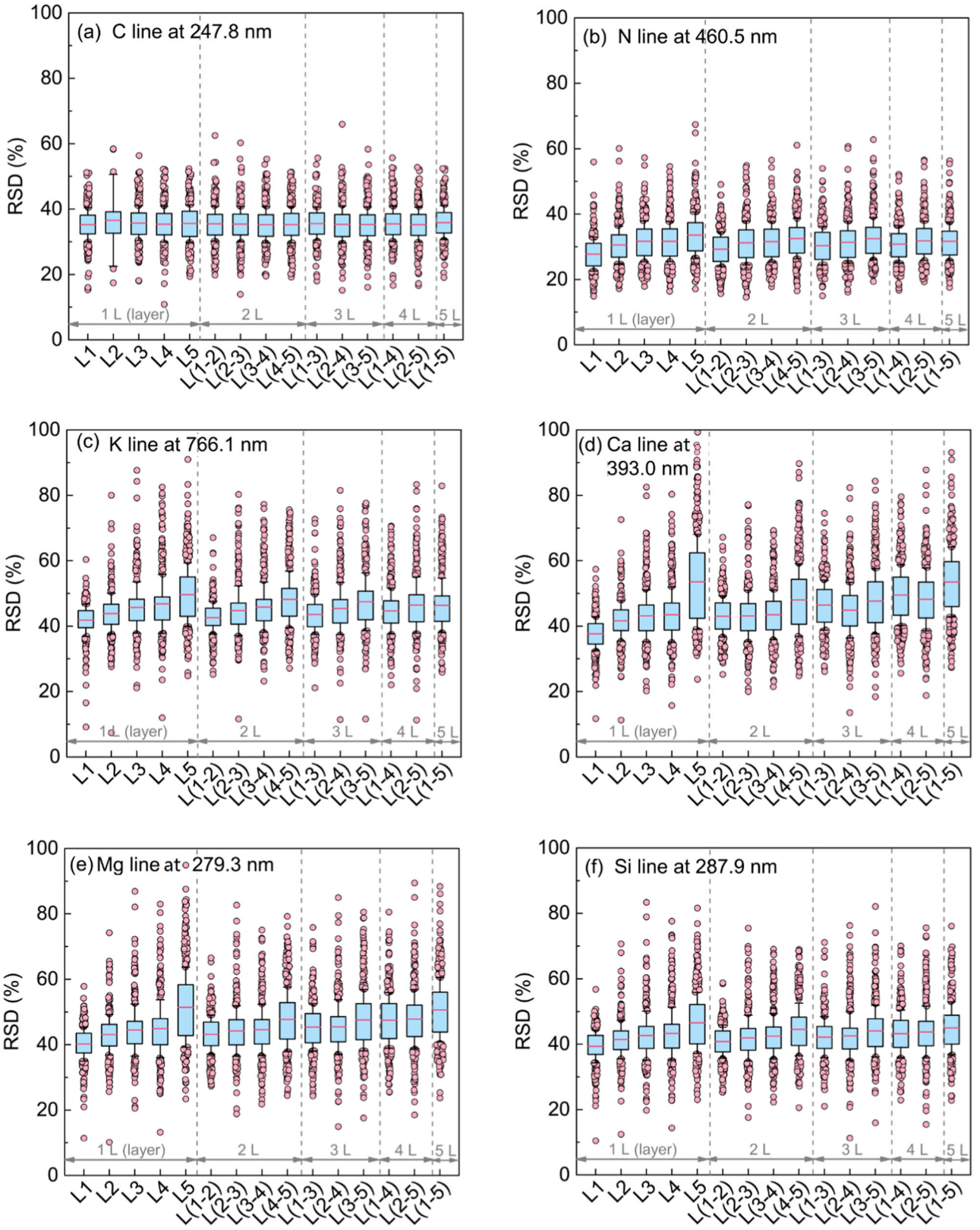

FIGURE 5 Boxplots of the RSD of (a) C, (b) N, (c) K, (d) Ca, (e) Mg, and (f) Si lines among 348 soil samples as a function of different shot layers. The number after "L" denotes the shot layer; shot number = 20; RSD is the relative standard deviation

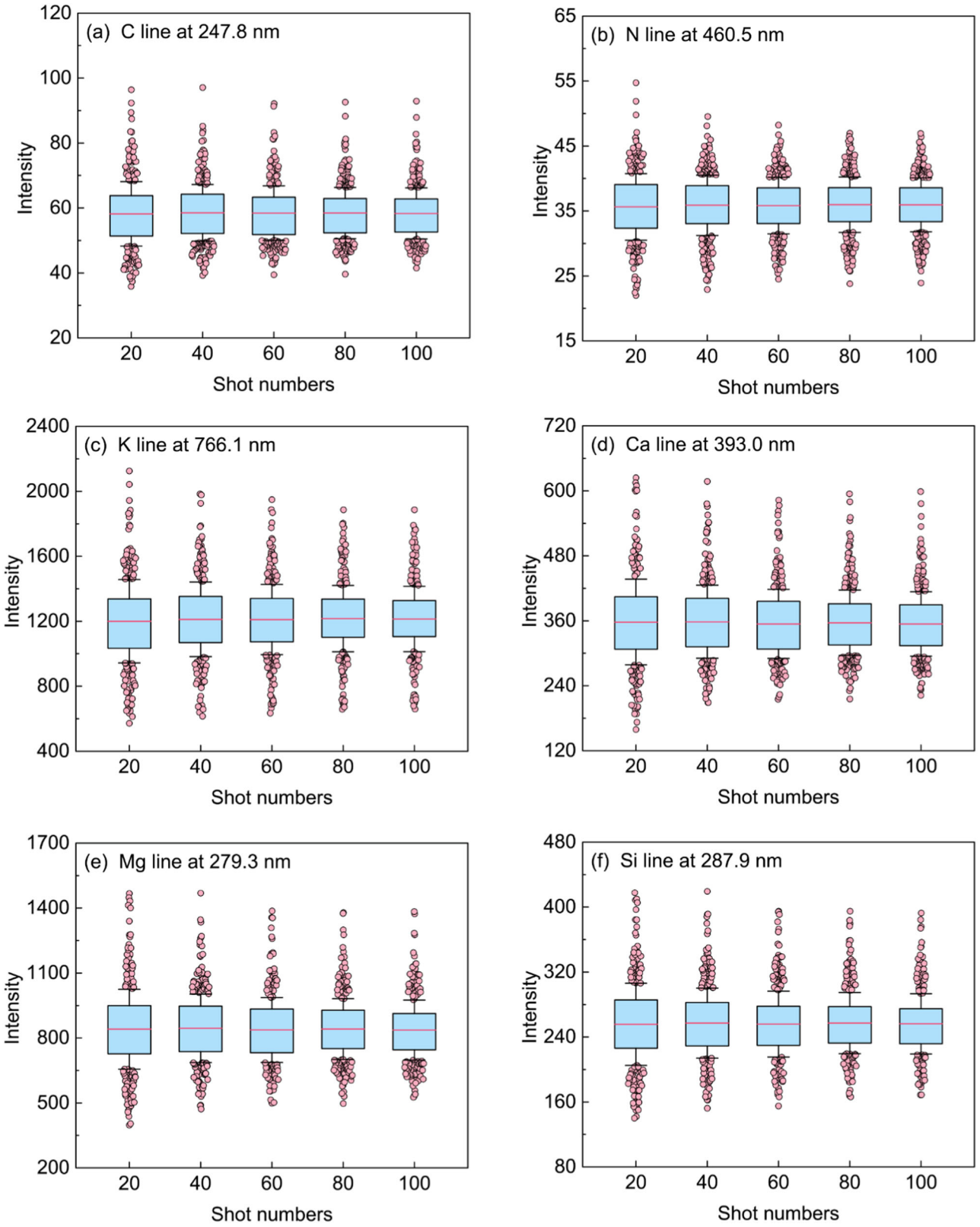

FIGURE 6 Boxplots of the (a) C, (b) N, (c) K, (d) Ca, (e) Mg, and (f) Si average intensities among 348 soil samples as a function of shot number. The shot layer was the 1st to 5th layers

(Figure 6), indicating that the variations of these spectral lines among these soil samples were lower at higher shot numbers. The shot number showed no obvious effect on the mean values of RSD in the 348 soil samples for C, N, K, Ca, Mg, and Si lines (Figure 7). The interquartile ranges and SD values of the RSD in these soil samples for C, N, K, Ca, Mg, and Si lines were markedly decreased along with the increase of shot number (Figure 7). Findings from these results indicated that increasing shot numbers were associated with a reduction in the spectral variation among these soil samples and provided a better and more robust estimate of the mean spectrum.

3.4 | Effects of the spectral acquisition and normalization approaches on the prediction accuracy of LIBS soil spectra

The influences of the shot layer on the $RMSE_V$ values for SOM, TN, and TSC in the validation set using PLSR based on full LIBS spectra from 200 to 1000 nm are depicted in Figure 8. Both the $RMSE_V$ values of SOM and TN decreased with increasing shot depth, suggesting that LIBS soil spectra at deeper shot layers were more favorable to the prediction of SOM and TN. Relatively lower $RMSE_V$ values of SOM and TN were observed for DN, DA, DM, and DS methods than for the AA method (Figure 8a, b), which indicated an improvement of LIBS quantitative abilities for SOM and TN by these methods. However, the $RMSE_V$ values of TSC increased with increasing shot depth. The DN, DA, DM, and DS methods reduced the quantitative accuracy of LIBS spectra for TSC, as the $RMSE_V$ values of TSC in these methods were higher than in the AA method.

The $RMSE_V$ values of SOM decreased markedly with increase in shot number except for the DS method (Figure 9a). When the shot number was 20, the DN, DA, DM, and DS methods showed higher SOM prediction accuracies than the AA method. When the shot number was 80 or 100, only the DM method showed higher SOM prediction accuracy than the AA method. For TN prediction, the DN, DA, DM, and DS methods showed lower $RMSE_V$ values than the AA method in various shot numbers (Figure 9b). This indicated that the DN, DA, DM, and DS methods dramatically improved the TN quantitative ability of LIBS soil spectra. With the increase of shot number, $RMSE_V$ values of TSC first decreased and then increased (Figure 9c). The optimal shot number was 40, where the DN, DA, DM, and DS methods showed no obvious improvement in TSC prediction accuracies of LIBS soil spectra.

The quantitative accuracies of LIBS soil spectra for SOM, TN, and TSC based on the combination of shot layer, shot number, and normalization methods were also investigated using the PLSR model. The statistics of prediction performances for SOM, TN, and TSC are listed in Supplemental Tables S1, S2, and S3, respectively. The optimal conditions for prediction of SOM, TN, and TSC were selected and the scatterplots of measured vs. predicted values and the VIP of variables are shown in Figure 10. The optimal model based on the approach of L5/SN20-DS showed fair performance for SOM prediction, with $RMSE_V$ of 2.076 g kg^{-1}, RPD_V of 1.608, and R_V^2 of 0.622. The higher VIP values for SOM predictions by LIBS spectra were mainly associated with the emission lines of C, O, N, K, Ca, and Mg elements (Figure 10b). The optimal model based on the approach of L4/SN20-DS presented good performance for TN prediction, with $RMSE_V$ of 0.123 g kg^{-1}, RPD_V of 1.836, and R_V^2 of 0.712. The higher VIP values for TN prediction in LIBS spectra were mainly located in the emission lines of C, N, O, K, Ca, and Mg elements (Figure 10d). The optimal model based on the approach of L(1-3)/SN60-AA showed very good performance for TSC prediction, with $RMSE_V$ of 0.581 g kg^{-1}, RPD_V of 2.456, and R_V^2 of 0.851. The higher VIP values for TSC prediction in LIBS spectra were mainly located in the emission lines of C, N, O, K, Ca, Si, Al, and Mg elements (Figure 10f).

3.5 | Correlation between the quality and the prediction accuracy of LIBS soil spectra

Spearman correlations between the $RMSE_V$ values of SOM, TN, and TSC and the RSD of various element lines (C, N, K, Ca, Mg, and Si) are given in Table 2. The correlation reflects the influence of the RSD values of various element lines on the quantitative accuracy. The negative correlation indicates that a lower RSD value is beneficial to improve the prediction accuracy and vice versa. For SOM, the $RMSE_V$ values in DM and DS methods showed a significant negative correlation with the RSD of C intensity. For TN, the $RMSE_V$ values in DN, DA, DM, and DS methods showed significant negative correlations with the RSD of N intensity. For TSC, the $RMSE_V$ values in the AA method showed a significant negative correlation with the RSD of N, K, Ca, Mg, and Si intensities. These results indicated that the RSD of LIBS spectra was a critical factor for quantitative accuracy of LIBS soil spectra.

4 | DISCUSSION

4.1 | Effect of the shot layer and number on the prediction accuracy of LIBS soil spectra

The sensibility of the measurement stability for LIBS is proven to be related to the LIBS parameters (Motto-Ros

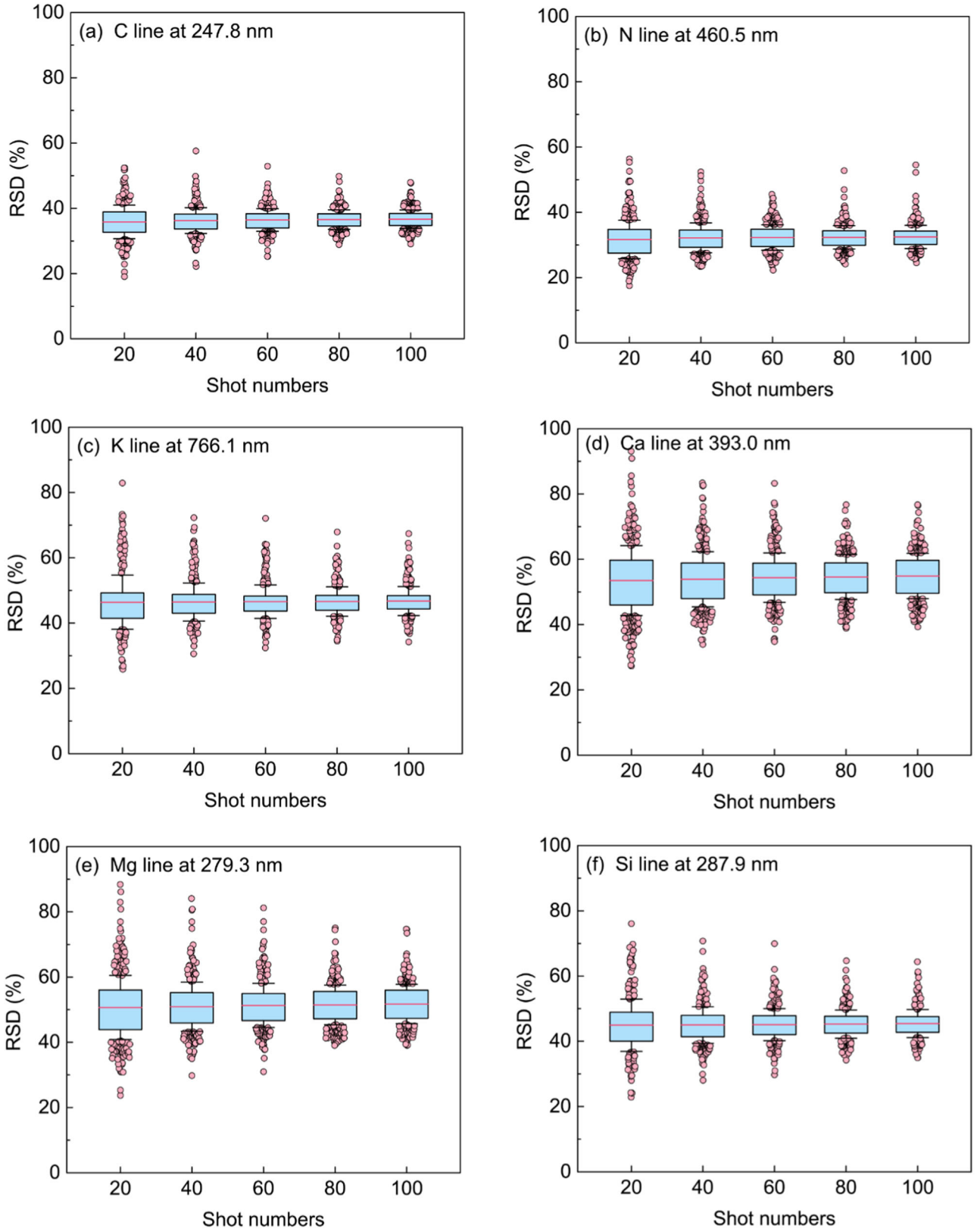

FIGURE 7 Boxplots of the RSD of the (a) C, (b) N, (c) K, (d) Ca, (e) Mg, and (f) Si intensities among 348 soil samples as the function of shot number. The shot layer was the 1st to 5th layers; RSD is the relative standard deviation

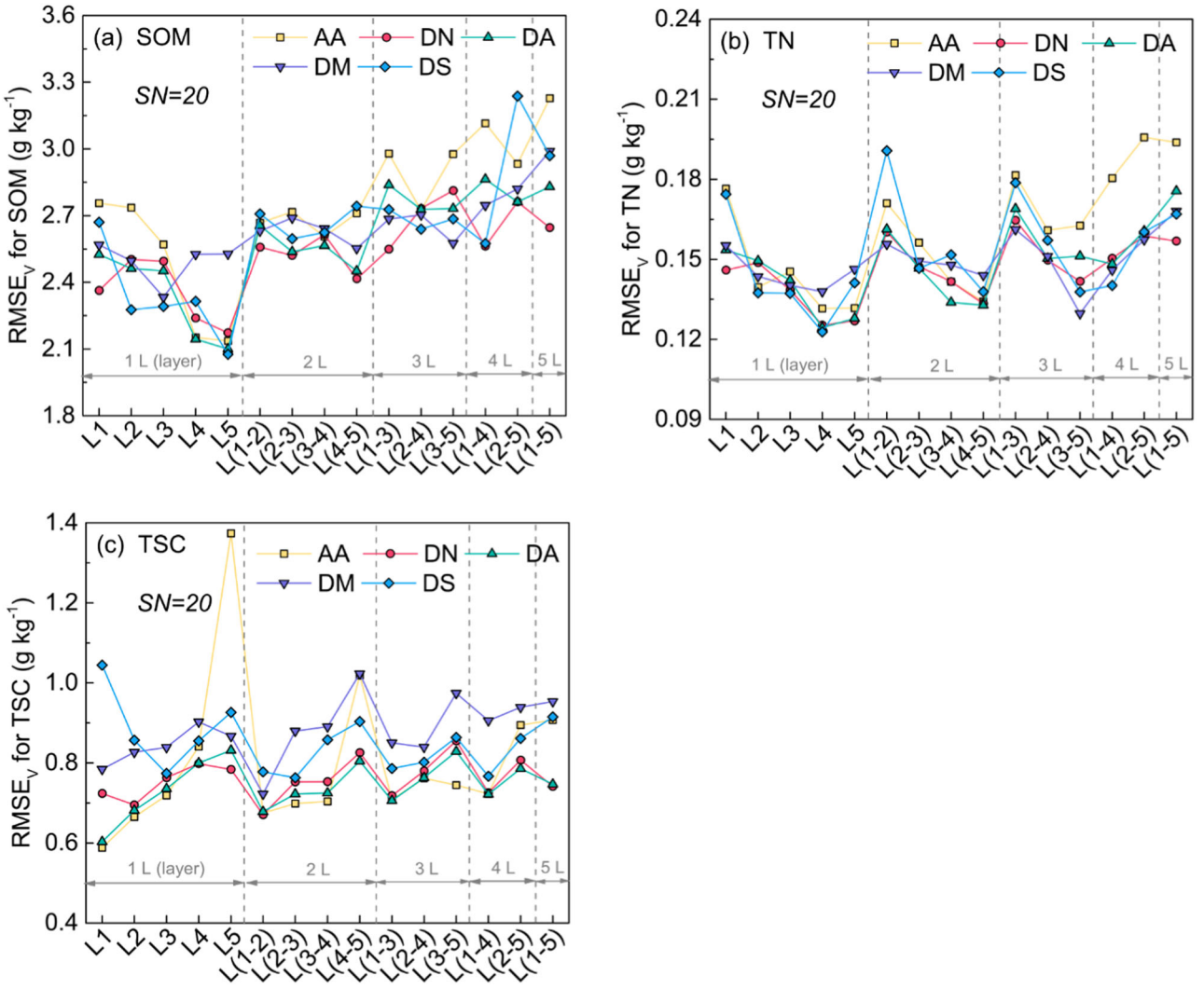

FIGURE 8 Changes of the root-mean-square-error of validation set ($RMSE_V$) values for (a) SOM, (b) TN, and (c) TSC based on various normalization methods along with shot layers. AA, arithmetic average method; DN, the method based on the correction of spectral norm; DA, the method based on the correction of spectral area; DM, the method based on the correction of spectral maximum; DS, the method based on the correction of Si line; the number after "L" denotes the shot layer; the shot number = 20

et al., 2014). For example, Castle, Talabardon, Smith, and Winefordner (1998) indicated that the RSD of the Cu emission signal decreased with increasing pulse energy. Zhang et al. (2010) showed that the 266-nm laser has lower RSD of spectra and better repeatability than 1064-nm laser. In this study, the LIBS parameters were controlled and unchanged; so the shot layer and number are two critical factors that influence the quantitative accuracy of LIBS soil spectra. The laser spot focused on the sample surface was limited to 50 μm in diameter, thereby only a small area of soil was ablated. Hence, the soil spectra were very sensitive to the uniformity of sample composition. However, the organic and inorganic components in the soil particle were unevenly distributed in mesoscopic (micron-sized) space because of soil heterogeneity (Barrios, Buresh, & Sprent, 1996). Consequently, the variation of the spectral signal at each site was very significant. Increasing the shot number could reduce the random errors of spectra caused by the soil heterogeneity and thereby improve the quantitative accuracy of LIBS soil spectra. The difference in the prediction accuracy of SOM, TN, and TSC by spectra of different shot layers could be caused by the uneven distribution of soil organic and inorganic components in the mesoscopic scale, which needs to be further analyzed and verified. When the laser ablates a specific site, particles are ejected owing to the pressure exerted by the plasma and the accompanying shock waves on melted layers (Noll, 2012). These particles collect in the crater as the shot depth increases (Noll, 2012). The energy of the laser pulses is partially absorbed by these loose particles, which decrease laser power density arriving at the bottom of the crater and thereby weaken the shock wave generated in the crater

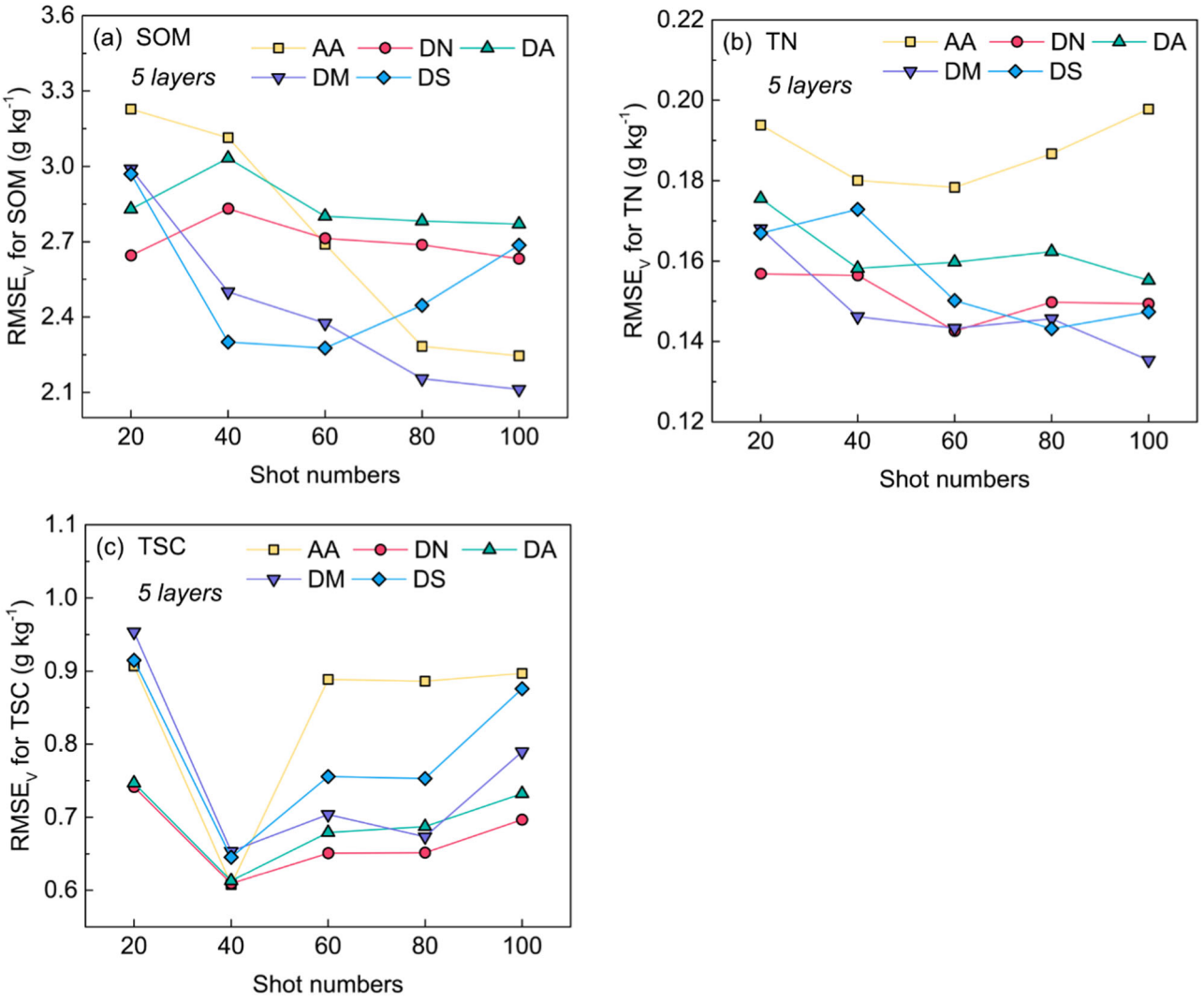

FIGURE 9 Changes of the root-mean-square-error of validation set ($RMSE_V$) values for (a) SOM, (b) TN, and (c) TSC based on various normalization methods against shot number. AA, arithmetic average method; DN, the method based on the correction of spectral norm; DA, the method based on the correction of spectral area; DM, the method based on the correction of spectral maximum; DS, the method based on the correction of Si line; the shot layer was the 1st to 5th layers

(Corsi et al., 2005; Pardede et al., 2009). As a result, in our study the intensities of the LIBS soil spectra decreased, and RSD of the intensities increased with increasing shot depth. Total soluble salt content is determined by the total amount of soluble HCO_3^-, CO_3^{2-}, Cl^-, SO_4^{2-}, Ca^{2+}, Mg^{2+}, K^+, and Na^+ in soil. As a consequence, the higher intensity of inorganic C, N, O, K, Ca, Mg, Al, and Si lines with surface shot layers was responsible for the better quantitative accuracies of TSC.

4.2 | Effects of normalization methods on the prediction accuracy of LIBS soil spectra

Applying different spectral normalization methods for different soil properties also could improve the quantitative accuracy of LIBS spectra. The DS method was optimal for the prediction of SOM and TN content. In the DS method, each multiple-measurement spectrum of one sample was first divided by its signal intensity of Si and then arithmetically averaged. In other words, this method assumes that the signal intensity of the Si line is undisturbed and invariable over multiple LIBS measurements. The success of the DS method at enhancing the accuracy of SOM and TN content prediction may be due to the following reason. Silicon is the second most abundant element in the earth's crust (Iler, 1979) and Si in free and combined forms is a dominant component of the solid material of many soils (McKeague & Cline, 1963). Thus, the variation in Si content in soil samples is small and consequently, the distribution of Si in the soil sample is relatively uniform (Martin, Wullschleger,

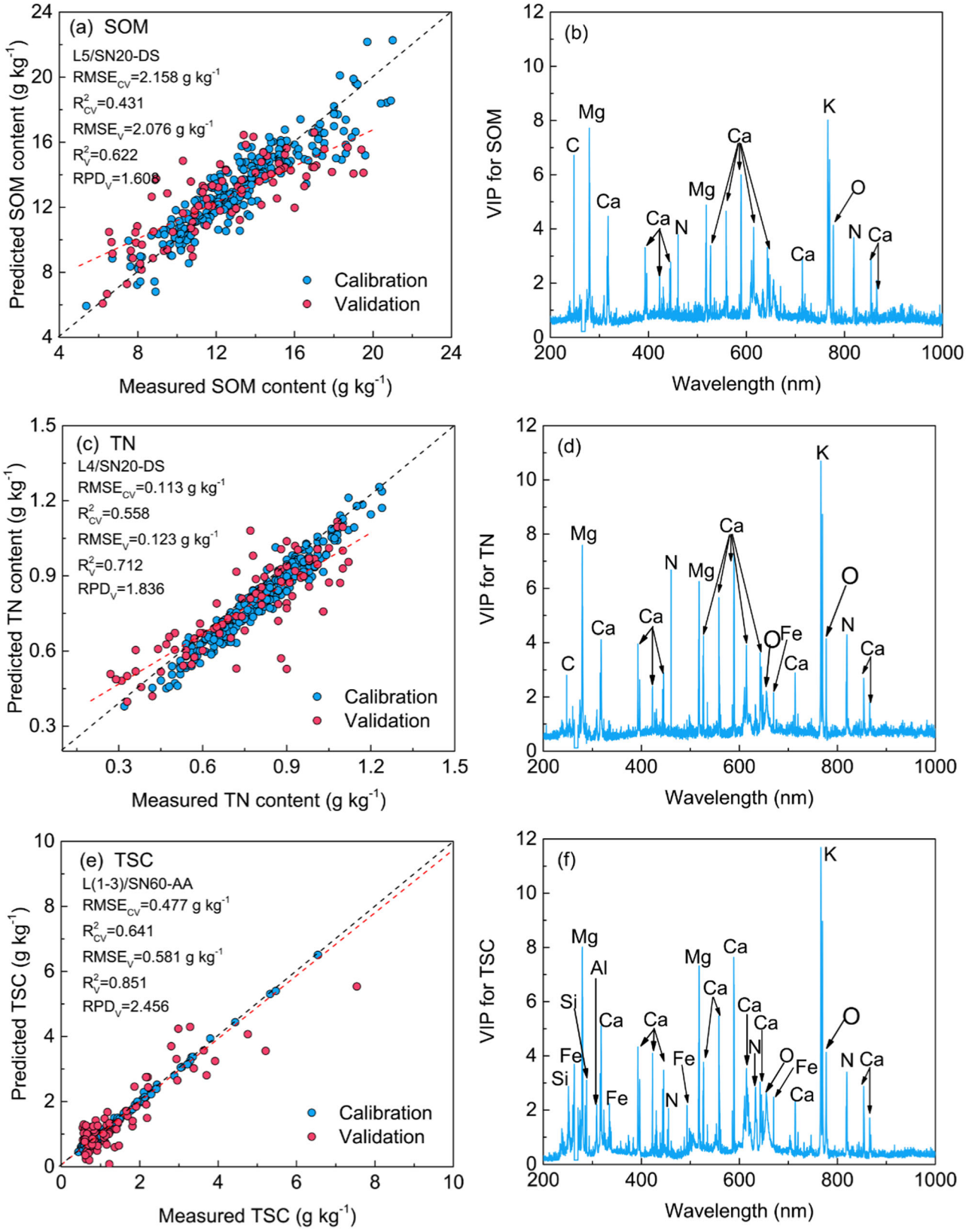

FIGURE 10 Scatterplots of measured vs. predicted values (a, c, and e) and the VIP plots of variables (b, d, f) for (a, b) SOM, (c and d) TN, and (e and f) TSC in PLSR models based on LIBS soil spectra under optimal conditions. Statistics are as follows: $RMSE_{CV}$ and $RMSE_V$ are the root-mean-square-error of 10-fold cross-validation and validation set, respectively; RPD_V is the residual prediction deviation of validation set; VIP is variable importance in projection

TABLE 2 Spearman correlation between the root-mean-square-error in the validation set ($RMSE_V$) of soil properties and the relative standard deviation (RSD) of characteristic spectral lines (nm) of elements using five normalization methods in 348 soil samples

Properties[a]	Normalization methods[b]	C 247.8	N 460.5	K 766.1	Ca 393.0	Mg 279.3	Si 287.9
SOM	AA	−0.146	−0.519**	−0.473**	0.039	−0.080	−0.230
	DN	0.022	−0.339*	−0.228	0.219	0.132	−0.004
	DA	0.227	−0.462*	−0.471**	0.311	0.159	−0.042
	DM	−0.557***	−0.657***	−0.459	−0.280	−0.361*	−0.460**
	DS	−0.367*	−0.292	−0.075	0.036	0.027	−0.069
TN	AA	0.136	−0.186	−0.221	0.457**	0.384*	0.180
	DN	0.178	−0.527**	−0.679***	0.078	−0.073	−0.289
	DA	0.292	−0.362*	−0.545***	0.200	0.086	−0.120
	DM	−0.347*	−0.544***	−0.491***	−0.147	−0.214	−0.342
	DS	−0.062	−0.570***	−0.561***	0.034	−0.052	−0.258
TSC	AA	−0.235	−0.463*	−0.777***	−0.385*	−0.490**	−0.640***
	DN	−0.684***	−0.003	0.313	−0.266	−0.172	−0.011
	DA	−0.481**	0.244	0.591***	0.104	0.204	0.362*
	DM	−0.610***	−0.052	0.253	−0.251	−0.205	−0.044
	DS	−0.307	0.100	0.192	−0.023	0.035	0.131

[a]SOM, soil organic matter; TN, total nitrogen; TSC, total soluble salt content

[b]AA, arithmetic average method; DN, the method based on the correction of spectral norm; DA, the method based on the correction of spectral area; DM, the method based on the correction of spectral maximum; DS, the method based on the correction of Si line

*Significant at the 0.05 probability level; **Significant at the 0.01 probability level; ***Significant at the 0.001 probability level

Garten, & Palumbo, 2003). Previous studies have also used the C/Si ratio method for improving LIBS accuracy (Cremers et al., 2001; Martin et al., 2003). However, these studies considered the small variation of Si content in all samples and applied the C/Si ratio method to spectra of all samples rather than multi-duplicated spectra of one sample. However, in practice, the Si content varies spatially for different soil samples (Bravo, Blanco, & Amiotti, 2007). In the present study, the SOM and TN content of soil samples ranged from 5.37 to 21.00 g kg^{-1} and 0.27 to 1.24 g kg^{-1}, respectively, and were significantly lower than Si content which was reported as 136 to 371 g kg^{-1} in Mollisols and Aridisols (Bravo et al., 2007). Consequently, the relatively weak signal intensities of C, H, O, and N were often inconsistent over repetitive measurements, resulting in the poor prediction accuracy of SOM and TN content by LIBS spectra. In the DS method, soil Si content was considered a useful 'internal standard' for correcting the other line intensities, because of the stability of the Si line in LIBS spectra. This also could be observed from the correlation between the $RMSE_V$ and RSD of various elements (Table 2). The negative correlation between the $RMSE_V$ and RSD of C or N intensity for SOM or TN was enhanced and the correlations between $RMSE_V$ and RSD of other lines were reduced after applying the DS method, suggesting that the DS method reduced the interferences of other lines and increased the sensitivity of the C line. These results indicated that the DS method can be considered as an effective normalization approach for improving the ability of LIBS spectra to predict SOM and TN content.

However, the DS method did not enhance the ability of LIBS spectra to predict TSC but actually impaired it. Among the five methods tested, the AA method was the most effective at enhancing TSC prediction. In the AA method, each multiple-measurement spectrum was directly averaged. The TSC values represented the mass sum of soluble K^+, Na^+, Ca^{2+}, Mg^{2+}, SO_4^{2-}, Cl^-, HCO_3^-, and CO_3^{2-}, which were related to the total content of these elements and the soil texture. The correlation between the $RMSE_V$ and RSD of N, K, Ca, Mg, and Si intensities were promoted after applying the AA method (Table 2), which also indicated the enhancement of the sensitivity of these lines. The content of these elements in the soil are comparable to the soil Si content. Therefore, using the DN, DA, DM, and DS methods for normalization of the multiple-measurement spectra might increase the signal intensity error of some elements related to TSC, resulting in a poor TSC prediction accuracy of LIBS spectra. The AA method was more effective for the TSC prediction by LIBS spectra than the other methods.

4.3 | Application of the LIBS technique to the quantitative analysis of farmland soil

Although LIBS is considered to be a well-established analytical technique, despite the large variety of experimental

designs and conditions, the treatment of LIBS spectra is often the subject of discussions and the suitability of this technique has not been sufficiently assessed (El Haddad, Canioni, & Bousquet, 2014). In soil science, advanced techniques for field analysis of soil properties should be capable of providing repetitive, sequential measurements for the evaluation of spatial and temporal variation (Segnini et al., 2014). The LIBS technique is superior to sequential measurements, but it lacks the advantage of repeatability because of the matrix effects of soil. Moreover, the lower SOM and TN content in these irrigated soils have negative effects on the accuracy of prediction using LIBS spectra. Many previous studies (Cremers et al., 2001; Martin et al., 2003; Senesi & Senesi, 2016) report considerable prediction accuracy for SOM content of soil using LIBS spectra, but these studies either used soils with higher SOM content or fewer soil samples. In our study, the SOM prediction accuracy (with R^2 of 0.622) was lower than the accuracy reported in previous studies with R^2 values of 0.96 (Cremers et al., 2001), 0.962 (Martin et al., 2003), 0.94 (Martin et al., 2010), and 0.94 (Glumac, Dong, & Jarrell, 2010). According to Bricklemyer, Brown, Turk, and Clegg (2018), LIBS shows better prediction performance for soil inorganic carbon than soil organic carbon. Thus, the lower prediction accuracy seen in our study may have been caused by higher carbonate content in the irrigated soil, which would seriously affect the accurate prediction of SOM content. Optimization of shot layer and number and normalization methods achieved fair, good, and very good as a predictor of SOM content, TN content, and TSC, respectively. Therefore, the LIBS technique combined with these optimization methods shows potential for simultaneously monitoring soil fertility and soil salinization or even other soil properties.

5 | CONCLUSIONS

There is an urgent need to develop simple, rapid, and convenient analytical techniques to the soil science. Laser-induced breakdown spectroscopy is a promising technique but is limited by low repeatability of spectral intensity which may influence the calibration results. In this study, we investigated the effects of shot layer and number as well as five spectral normalization approaches on the qualities and quantitative abilities of LIBS soil spectra using PLSR models. Increasing shot number improved the estimated robustness of the mean LIBS spectrum, thereby increasing the prediction accuracies of SOM, TN, and TSC. Spectra of deep shot layers (4th or 5th shot layer) in soil samples provided higher prediction accuracies for SOM and TN content and lower prediction accuracy for TSC than that of surface shot layers (1st and 2nd shot layer). Applying the DS normalization method to soil spectra markedly improved the prediction accuracies of SOM and TN by reducing the interferences of other lines. The AA normalization method showed better prediction performance for TSC than other methods. Findings from this work indicated that optimization of spectral acquisition and normalization approaches significantly enhanced the prediction accuracy of LIBS soil spectra, providing a novel strategy for future application.

ACKNOWLEDGMENTS

The work was supported by the National Natural Science Foundation of China (41671238, 41977026), and the Jiangsu Demonstration Project in Modern Agriculture (BE2017388), and the "STS" Project from Chinese Academy of Sciences (KFJ-PTXM-003, KFJ-STS-QYZX-047).

ORCID

Changwen Du https://orcid.org/0000-0002-9064-3581

REFERENCES

Abdel-Salam, Z., Al Sharnoubi, J., & Harith, M. A. (2013). Qualitative evaluation of maternal milk and commercial infant formulas via LIBS. *Talanta*, *115*, 422–426. https://doi.org/10.1016/j.talanta.2013.06.003

Ahmed, N., Umar, Z. A., Ahmed, R., & Baig, M. A. (2017). On the elemental analysis of different cigarette brands using laser induced breakdown spectroscopy and laser-ablation time of flight mass spectrometry. *Spectrochimica Acta Part B: Atomic Spectroscopy*, *136*, 39–44. https://doi.org/10.1016/j.sab.2017.08.006

Barrios, E., Buresh, R. J., & Sprent, J. I. (1996). Organic matter in soil particle size and density fractions from maize and legume cropping systems. *Soil Biology & Biochemistry*, *28*(2), 185–193. https://doi.org/10.1016/0038-0717(95)00110-7

Body, D., & Chadwick, B. L. (2001). Optimization of the spectral data processing in a LIBS simultaneous elemental analysis system. *Spectrochimica Acta Part B: Atomic Spectroscopy*, *56*(6), 725–736. https://doi.org/10.1016/S0584-8547(01)00186-0

Bravo, O., Blanco, M. C., & Amiotti, N. (2007). Control factors in the segregation of Mollisols and Aridisols of the semiarid–arid transition of Argentina. *Catena*, *70*(2), 220–228. https://doi.org/10.1016/j.catena.2006.08.008

Bricklemyer, R. S., Brown, D. J., Turk, P. J., & Clegg, S. (2018). Comparing vis–NIRS, LIBS, and combined vis–NIRS-LIBS for intact soil core soil carbon measurement. *Soil Science Society of America Journal*, *82*(6), 1482–1496. https://doi.org/10.2136/sssaj2017.09.0332

Castle, B. C., Talabardon, K., Smith, B. W., & Winefordner, J. D. (1998). Variables influencing the precision of laser-induced breakdown spectroscopy measurements. *Applied Spectroscopy*, *52*(5), 649–657. https://doi.org/10.1366/0003702981944300

Castro, J. P., & Pereira-Filho, E. R. (2016). Twelve different types of data normalization for the proposition of classification, univariate and multivariate regression models for the direct analyses of alloys by laser-induced breakdown spectroscopy (LIBS). *Journal of Analytical Atomic Spectrometry*, *31*(10), 2005–2014. https://doi.org/10.1039/C6JA00224B

Chen, H., Huo, Z., Dai, X., Ma, S., Xu, X., & Huang, G. (2018). Impact of agricultural water-saving practices on regional evapotranspiration: The role of groundwater in sustainable agriculture in arid and semi-arid areas. *Agricultural and Forest Meteorology*, *263*, 156–168. https://doi.org/10.1016/j.agrformet.2018.08.013

Corsi, M., Cristoforetti, G., Hidalgo, M., Iriarte, D., Legnaioli, S., Palleschi, V., … Tognoni, E. (2005). Effect of laser-induced crater depth in laser-induced breakdown spectroscopy emission features. *Applied Spectroscopy*, *59*(7), 853–860. https://doi.org/10.1366/0003702054411607

Cremers, D. A., Ebinger, M. H., Breshears, D. D., Unkefer, P. J., Kammerdiener, S. A., Ferris, M. J., … Brown, J. R. (2001). Measuring total soil carbon with laser-induced breakdown spectroscopy (LIBS). *Journal of Environmental Quality*, *30*(6), 2202–2206. https://doi.org/10.2134/jeq2001.2202

De Lucia Jr, F. C., & Gottfried, J. L. (2010). Characterization of a series of nitrogen-rich molecules using laser induced breakdown spectroscopy. *Propellants, Explosives, Pyrotechnics*, *35*(3), 268–277. https://doi.org/10.1002/prep.201000009

Dong, D. M., Zhao, C. J., Zheng, W. G., Zhao, X. D., & Jiao, L. Z. (2013). Spectral characterization of nitrogen in farmland soil by laser-induced breakdown spectroscopy. *Spectroscopy Letters*, *46*(6), 421–426. https://doi.org/10.1080/00387010.2012.747542

Du, C., Ma, Z., Zhou, J., & Goyne, K. W. (2013). Application of mid-infrared photoacoustic spectroscopy in monitoring carbonate content in soils. *Sensors and Actuators B: Chemical*, *188*, 1167–1175. https://doi.org/10.1016/j.snb.2013.08.023

El Haddad, J., Canioni, L., & Bousquet, B. (2014). Good practices in LIBS analysis: Review and advices. *Spectrochimica Acta Part B: Atomic Spectroscopy*, *101*, 171–182. https://doi.org/10.1016/j.sab.2014.08.039

Eppler, A. S., Cremers, D. A., Hickmott, D. D., Ferris, M. J., & Koskelo, A. C. (1996). Matrix effects in the detection of Pb and Ba in soils using laser-induced breakdown spectroscopy. *Applied Spectroscopy*, *50*(9), 1175–1181. https://doi.org/10.1366/0003702963905123

Farrés, M., Platikanov, S., Tsakovski, S., & Tauler, R. (2015). Comparison of the variable importance in projection (VIP) and of the selectivity ratio (SR) methods for variable selection and interpretation. *Journal of Chemometrics*, *29*(10), 528–536. https://doi.org/10.1002/cem.2736

Feng, Z. Z., Wang, X. K., & Feng, Z. W. (2005). Soil N and salinity leaching after the autumn irrigation and its impact on groundwater in Hetao Irrigation District, China. *Agricultural Water Management*, *71*(2), 131–143. https://doi.org/10.1016/j.agwat.2004.07.001

Ferreira, E. C., Neto, J. A. G., Milori, D. M. B. P., Ferreira, E. J., & Anzano, J. M. (2015). Laser-induced breakdown spectroscopy: Extending its application to soil pH measurements. *Spectrochimica Acta Part B: Atomic Spectroscopy*, *110*, 96–99. https://doi.org/10.1016/j.sab.2015.06.002

Fu, Y., Hou, Z., Li, T., Li, Z., & Wang, Z. (2019). Investigation of intrinsic origins of the signal uncertainty for laser-induced breakdown spectroscopy. *Spectrochimica Acta Part B: Atomic Spectroscopy*, *155*, 67–78. https://doi.org/10.1016/j.sab.2019.03.007

Glumac, N. G., Dong, W. K., & Jarrell, W. M. (2010). Quantitative analysis of soil organic carbon using laser-induced breakdown spectroscopy: An improved method. *Soil Science Society of America Journal*, *74*, 1922–1928. https://doi.org/10.2136/sssaj2010.0100

Hao, Z., Liu, L., Shen, M., Zhou, R., Li, J., Guo, L., … Zeng, X. (2018). Long-term repeatability improvement of quantitative LIBS using a two-point standardization method. *Journal of Analytical Atomic Spectrometry*, *33*(9), 1564–1570. https://doi.org/10.1039/C8JA00148K

Harris, R. D., Cremers, D. A., Ebinger, M. H., & Bluhm, B. K. (2004). Determination of nitrogen in sand using laser-induced breakdown spectroscopy. *Applied Spectroscopy*, *58*(7), 770–775. https://doi.org/10.1366/0003702041389201

Iler, P. K. (1979). *The chemistry of silica*. New York: Wiley and Sons.

Ismail, M. A., Cristoforetti, G., Legnaioli, S., Pardini, L., Palleschi, V., Salvetti, A., … Harith, M. A. (2006). Comparison of detection limits, for two metallic matrices, of laser-induced breakdown spectroscopy in the single and double-pulse configurations. *Analytical and Bioanalytical Chemistry*, *385*(2), 316–325. https://doi.org/10.1007/s00216-006-0363-z

Ji, W., Adamchuk, V. I., Chen, S., Su, A. S. M., Ismail, A., Gan, Q., … Biswas, A. (2019). Simultaneous measurement of multiple soil properties through proximal sensor data fusion: A case study. *Geoderma*, *341*, 111–128. https://doi.org/10.1016/j.geoderma.2019.01.006

Ji, Z. G., Xi, J. H., & Mao, Q. N. (2010). Determination of oxygen concentration in heavily doped silicon wafer by laser induced breakdown spectroscopy. *Journal of Inorganic Materials*, *25*(8), 893–895. https://doi.org/10.3724/SP.J.1077.2010.10074

Juvé, V., Portelli, R., Boueri, M., Baudelet, M., & Yu, J. (2008). Space-resolved analysis of trace elements in fresh vegetables using ultraviolet nanosecond laser-induced breakdown spectroscopy. *Spectrochimica Acta Part B: Atomic Spectroscopy*, *63*(10), 1047–1053. https://doi.org/10.1016/j.sab.2008.08.009

Knadel, M., Gislum, R., Hermansen, C., Peng, Y., Moldrup, P., de Jonge, L. W., & Greve, M. H. (2017). Comparing predictive ability of laser-induced breakdown spectroscopy to visible near-infrared spectroscopy for soil property determination. *Biosystems Engineering*, *156*, 157–172. https://doi.org/10.1016/j.biosystemseng.2017.01.007

Lao, J. S. (1988). *Handbook of soil and agricultural chemistry analysis*. Beijing: Agricultural Press.

Lei, T., Issac, S., Yuan, P., Huang, X., & Yang, P. (2001). Strategic considerations of efficient irrigation and salinity control on Hetao Plain in inner Mongolia. *Nongye Gongcheng Xuebao (Transactions of the Chinese Society of Agricultural Engineering)*, *17*(1), 48–52. https://doi.org/10.3321/j.issn:1002-6819.2001.01.010

Li, H. K., Liu, M., Chen, Z. J., & Li, R. H. (2008). Quantitative analysis of impurities in aluminum alloys by laser-induced breakdown spectroscopy without internal calibration. *Transactions of Nonferrous Metals Society of China*, *18*(1), 222–226. https://doi.org/10.1016/S1003-6326(08)60040-0

Li, Z., Zhan, D. J., Wang, J. J., Huang, J., Xu, Q. S., Zhang, Z. M., … Wang, H. (2013). Morphological weighted penalized least squares for background correction. *Analyst*, *138*(16), 4483–4492. https://doi.org/10.1039/C3AN00743J

Liu, L. W., Zeng, W. L., Zhang, J. L., Liu, L. M., & Lin, Z. X. (2012). Cation exchange detection in the process of ionic soil stabilizer reinforcing soil by laser-induced breakdown spectroscopy. *Advances in Materials Research*, *510*, 799–803. https://doi.org/10.4028/www.scientific.net/AMR.510.799

Lu, C., Wang, L., Hu, H., Zhuang, Z., Wang, Y., Wang, R., & Song, L. (2013). Analysis of total nitrogen and total phosphorus in soil

using laser-induced breakdown spectroscopy. *Chinese Optics Letters*, *11*(5), 053004.

Lu, Y., Du, C., Yu, C., & Zhou, J. (2014). Fast and nondestructive determination of protein content in rapeseeds (*Brassica napus* L.) using Fourier transform infrared photoacoustic spectroscopy (FTIR-PAS). *Journal of the Science of Food and Agriculture*, *94*(11), 2239–2245. https://doi.org/10.1002/jsfa.6548

Luna, A. S., Gonzaga, F. B., da Rocha, W. F. C., & Lima, I. C. A. (2018). A comparison of different strategies in multivariate regression models for the direct determination of Mn, Cr, and Ni in steel samples using laser-induced breakdown spectroscopy. *Spectrochimica Acta Part B: Atomic Spectroscopy*, *139*, 20–26. https://doi.org/10.1016/j.sab.2017.10.016

Ma, F., Du, C., & Zhou, J. (2016). A self-adaptive model for the prediction of soil organic matter using mid-infrared photoacoustic spectroscopy. *Soil Science Society of America Journal*, *80*(1), 238–246. https://doi.org/10.2136/sssaj2015.06.0234

Ma, F., Du, C. W., Zhou, J. M., & Shen, Y. Z. (2019). Investigation of soil properties using different techniques of mid-infrared spectroscopy. *European Journal of Soil Science*, *70*(1), 96–106. https://doi.org/10.1111/ejss.12741

Mansoori, A., Roshanzadeh, B., Khalaji, M., & Tavassoli, S. H. (2011). Quantitative analysis of cement powder by laser induced breakdown spectroscopy. *Optics & Lasers in Engineering*, *49*(3), 318–323. https://doi.org/10.1016/j.optlaseng.2010.10.005

Martin, M. Z., Labbé, N., André, N., Wullschleger, S. D., Harris, R. D., & Ebinger, M. H. (2010). Novel multivariate analysis for soil carbon measurements using laser-induced breakdown spectroscopy. *Soil Science Society of America Journal*, *74*(1), 87–93. https://doi.org/10.2136/sssaj2009.0102

Martin, M. Z., Wullschleger, S. D., Garten, C. T., & Palumbo, A. V. (2003). Laser-induced breakdown spectroscopy for the environmental determination of total carbon and nitrogen in soils. *Applied Optics*, *42*(12), 2072–2077. https://doi.org/10.1364/AO.42.002072

McKeague, J. A., & Cline, M. G. (1963). Silica in soils. *Advances in Agronomy*, *15*, 339–396. https://doi.org/10.1016/S0065-2113(08)60403-4

Michel, A. P. M., & Chave, A. D. (2007). Analysis of laser-induced breakdown spectroscopy spectra: The case for extreme value statistics. *Spectrochimica Acta Part B: Atomic Spectroscopy*, *62*(12), 1370–1378. https://doi.org/10.1016/j.sab.2007.10.027

Motto-Ros, V., Negre, E., Pelascini, F., Panczer, G., & Yu, J. (2014). Precise alignment of the collection fiber assisted by real-time plasma imaging in laser-induced breakdown spectroscopy. *Spectrochimica Acta Part B: Atomic Spectroscopy*, *92*, 60–69. https://doi.org/10.1016/j.sab.2013.12.008

Nguyen, H. V.-M., Moon, S. J., & Choi, J. H. (2015). Improving the application of laser-induced breakdown spectroscopy for the determination of total carbon in soils. *Environmental Monitoring and Assessment*, *187*(2), 28. https://doi.org/10.1007/s10661-015-4286-z

Noll, R. (2012). *Laser-induced breakdown spectroscopy: Fundamentals and applications*. Heidelberg, Germany: Springer-Verlag.

Pansu, M., & Gautheyrou, J. (2007). *Handbook of soil analysis mineralogical, organic and inorganic methods*. Heidelberg, Germany: Springer-Verlag.

Pardede, M., Lie, T. J., Kurniawan, K. H., Niki, H., Fukumoto, K., Maruyama, T., … Tjia, M. O. (2009). Crater effects on H and D emission from laser induced low-pressure helium plasma. *Journal of Applied Physics*, *106*(6), 063303. https://doi.org/10.1063/1.3224864

Paules, D., Hamida, S., Lasheras, R. J., Escudero, M., Benouali, D., Cáceres, J. O., & Anzano, J. (2018). Characterization of natural and treated diatomite by laser-induced breakdown spectroscopy (LIBS). *Microchemical Journal*, *137*, 1–7. https://doi.org/10.1016/j.microc.2017.09.020

Peltre, C., Bruun, S., Du, C., Thomsen, I. K., & Jensen, L. S. (2014). Assessing soil constituents and labile soil organic carbon by mid-infrared photoacoustic spectroscopy. *Soil Biology & Biochemistry*, *77*, 41–50. https://doi.org/10.1016/j.soilbio.2014.06.022

Rai, A. K., Zhang, H., Yueh, F. Y., Singh, J. P., & Weisberg, A. (2001). Parametric study of a fiber-optic laser-induced breakdown spectroscopy probe for analysis of aluminum alloys. *Spectrochimica Acta Part B: Atomic Spectroscopy*, *56*(12), 2371–2383. https://doi.org/10.1016/S0584-8547(01)00299-3

Sabsabi, M., Detalle, V., Harith, M. A., Tawfik, W., & Imam, H. (2003). Comparative study of two new commercial echelle spectrometers equipped with intensified CCD for analysis of laser-induced breakdown spectroscopy. *Applied Optics*, *42*(30), 6094–6098. https://doi.org/10.1364/AO.42.006094

Sallé, B., Cremers, D. A., Maurice, S., Wiens, R. C., & Fichet, P. (2005). Evaluation of a compact spectrograph for in-situ and stand-off laser-induced breakdown spectroscopy analyses of geological samples on Mars missions. *Spectrochimica Acta Part B: Atomic Spectroscopy*, *60*(6), 805–815. https://doi.org/10.1016/j.sab.2005.05.007

Segnini, A., Xavier, A. A. P., Otaviani-Junior, P. L., Ferreira, E. C., Watanabe, A. M., Sperança, M. A., … Milori, D. M. B. P. (2014). Physical and chemical matrix effects in soil carbon quantification using laser-induced breakdown spectroscopy. *American Journal of Analytical Chemistry*, *5*, 722–729. https://doi.org/10.4236/ajac.2014.511080

Senesi, G. S. (2014). Laser-induced Breakdown Spectroscopy (LIBS) applied to terrestrial and extraterrestrial analogue geomaterials with emphasis to minerals and rocks. *Earth-Science Reviews*, *139*, 231–267. https://doi.org/10.1016/j.earscirev.2014.09.008

Senesi, G. S., & Senesi, N. (2016). Laser-induced breakdown spectroscopy (LIBS) to measure quantitatively soil carbon with emphasis on soil organic carbon. *Analytica Chimica Acta*, *938*, 7–17. https://doi.org/10.1016/j.aca.2016.07.039

Sirven, J.-B., Mauchien, P., & Sallé, B. (2008). Analytical optimization of some parameters of a laser-induced breakdown spectroscopy experiment. *Spectrochimica Acta Part B: Atomic Spectroscopy*, *63*(10), 1077–1084. https://doi.org/10.1016/j.sab.2008.08.013

Takahashi, T., & Thornton, B. (2017). Quantitative methods for compensation of matrix effects and self-absorption in laser induced breakdown spectroscopy signals of solids. *Spectrochimica Acta Part B: Atomic Spectroscopy*, *138*, 31–42. https://doi.org/10.1016/j.sab.2017.09.010

Velioglu, H. M., Sezer, B., Bilge, G., Baytur, S. E., & Boyaci, I. H. (2018). Identification of offal adulteration in beef by laser induced breakdown spectroscopy (LIBS). *Meat Science*, *138*, 28–33. https://doi.org/10.1016/j.meatsci.2017.12.003

Villas-Boas, P. R., Romano, R. A., de Menezes Franco, M. A., Ferreira, E. C., Ferreira, E. J., Crestana, S., & Milori, D. M. B. P. (2016). Laser-induced breakdown spectroscopy to determine soil texture: A fast analytical technique. *Geoderma*, *263*, 195–202. https://doi.org/10.1016/j.geoderma.2015.09.018

Rossel, Viscarra, A., R., McGlynn, R. N., & McBratney, A. B. (2006). Determining the composition of mineral-organic mixes using UV–vis–NIR diffuse reflectance spectroscopy. *Geoderma*, *137*(1–2), 70–82. https://doi.org/10.1016/j.geoderma.2006.07.004

Wainner, R. T., Harmon, R. S., Miziolek, A. W., McNesby, K. L., & French, P. D. (2001). Analysis of environmental lead contamination: Comparison of LIBS field and laboratory instruments. *Spectrochimica Acta Part B: Atomic Spectroscopy*, *56*(6), 777–793. https://doi.org/10.1016/S0584-8547(01)00229-4

Walkley, A., & Black, I. A. (1934). An examination of Degtjareff method for determining soil organic matter, and a proposed modification of the chromic acid titration method. *Soil Science*, *37*(1), 29–38. https://doi.org/10.1097/00010694-193401000-00003

Wold, S., Sjöström, M., & Eriksson, L. (2001). PLS-regression: A basic tool of chemometrics. *Chemometrics Intelligent Laboratory Systems*, *58*(2), 109–130. https://doi.org/10.1016/S0169-7439(01)00155-1

Xing, Z., Du, C., Tian, K., Ma, F., Shen, Y., & Zhou, J. (2016). Application of FTIR-PAS and Raman spectroscopies for the determination of organic matter in farmland soils. *Talanta*, *158*, 262–269. https://doi.org/10.1016/j.talanta.2016.05.076

Yamamoto, K. Y., Cremers, D. A., Ferris, M. J., & Foster, L. E. (1996). Detection of metals in the environment using a portable laser-induced breakdown spectroscopy instrument. *Applied Spectroscopy*, *50*(2), 222–233. https://doi.org/10.1366/0003702963906519

Yang, Y., Shang, S., & Jiang, L. (2012). Remote sensing temporal and spatial patterns of evapotranspiration and the responses to water management in a large irrigation district of North China. *Agricultural and Forest Meteorology*, *164*, 112–122. https://doi.org/10.1016/j.agrformet.2012.05.011

Yaroshchyk, P., Morrison, R. J. S., Body, D., & Chadwick, B. L. (2005). Quantitative determination of wear metals in engine oils using laser-induced breakdown spectroscopy: A comparison between liquid jets and static liquids. *Spectrochimica Acta Part B: Atomic Spectroscopy*, *60*(7-8), 986–992. https://doi.org/10.1016/j.sab.2005.03.011

Yu, R., Liu, T., Xu, Y., Zhu, C., Zhang, Q., Qu, Z., … Li, C. (2010). Analysis of salinization dynamics by remote sensing in Hetao Irrigation District of North China. *Agricultural and Forest Meteorology*, *97*, 1952–1960. https://doi.org/10.1016/j.agwat.2010.03.009

Yue, Y., Guo, W. N., Lin, Q. M., Li, G. T., & Zhao, X. R. (2016). Improving salt leaching in a simulated saline soil column by three biochars derived from rice straw (*Oryza sativa* L.), sunflower straw (*Helianthus annuus*), and cow manure. *Journal of Soil and Water Conservation*, *71*(6), 467–475. https://doi.org/10.2489/jswc.71.6.467

Zaytsev, S. M., Krylov, I. N., Popov, A. M., Zorov, N. B., & Labutin, T. A. (2018). Accuracy enhancement of a multivariate calibration for lead determination in soils by laser induced breakdown spectroscopy. *Spectrochimica Acta Part B: Atomic Spectroscopy*, *140*, 65–72. https://doi.org/10.1016/j.sab.2017.12.005

Zhang, D. C., Ma, X. W., Wen, W. Q. W., Zhang, P. J., Zhu, X. L., Li, B., & Liu, H. P. (2010). Influence of laser wavelength on laser-induced breakdown spectroscopy applied to semi-quantitative analysis of trace-elements in a plant sample. *Chinese Physics Letters*, *27*(6), 063202. https://doi.org/10.1088/0256-307X/27/6/063202

Zheng, H., Yueh, F. Y., Miller, T., Singh, J. P., Zeigler, K. E., & Marra, J. C. (2008). Analysis of plutonium oxide surrogate residue using laser-induced breakdown spectroscopy. *Spectrochimica Acta Part B: Atomic Spectroscopy*, *63*(9), 968–974. https://doi.org/10.1016/j.sab.2008.06.005

SUPPORTING INFORMATION

Additional supporting information may be found online in the Supporting Information section at the end of the article.

How to cite this article: Xu X, Du C, Ma F, Shen Y, Zhang Y, Zhou J. Optimization of measuring procedure of farmland soils using laser-induced breakdown spectroscopy. *Soil Sci. Soc. Am. J.* 2020;84:1307–1326. https://doi.org/10.1002/saj2.20071